A NEW METHOD OF PARAMETER IDENTIFICATION FOR PROTON EXCHANGE MEMBRANE FUEL CELL BASED ON HYBRID PARTICLE SWARM OPTIMIZATION WITH DIFFERENTIAL EVOLUTION ALGORITHM

by

Dong LIU, Xiangguo YANG, Cong GUAN*, Tianxi QI, and Qinggen ZHENG

Key Laboratory of High Performance Ship Technology of Ministry of Education,
Wuhan University of Technology, Wuhan, China

Original scientific paper
https://doi.org/10.2298/TSCI220912062L

With the characteristics of high energy conversion efficiency, high energy density and low operating temperature, the proton exchange membrane fuel cells (PEMFC) have become one of the green energy sources with broad prospects. The establishment of accurate mathematical model of the PEMFC is the basis of simulation and control strategy. At present, some intelligent algorithms have certain drawbacks, and can hardly find the balanced point between precision and computational time. In this study, a novel parameter identification approach combining the hybrid particle swarm optimization (PSO) algorithm with differential evolution, i.e. hybrid DEPSO, is proposed to obtain the unknown parameters in the PEMFC mathematical model and solve the problems of premature convergence of PSO and poor global search ability of differential evolution. Six benchmark functions are applied to verify the performance of the algorithm. The results prove that the hybrid DEPSO can evade local optimum preferably while having swifter convergence rate. Two PEMFC stacks are investigated and modeled. In order to evaluate the accuracy of model, the sum of squared errors between the measured voltage and the estimated output voltage are examined. Numerical results show higher accuracy of the hybrid DEPSO-based model comparing with other recently published optimization approaches. Furthermore, the simulation results indicate that the accuracy of the PEMFC model optimized by the hybrid DEPSO algorithm improves 0.19-1.86%, which can provide a new solution the multi-objective optimization problem and promote the practical application of the PEMFC.

Key words: *PEMFC, parameters identification, PSO algorithm, differential evolution algorithm*

Introduction

Ships typically use Diesel engines as power source, which produce a large amount of SO_x, CO_2 and particulate matter, causing damage to the environment. Compared with other traditional energy sources, hydrogen energy is a reliable, efficient and durable energy source that continuously converts input hydrogen into electricity [1]. Hence, hydrogen energy and fuel cell technology is a major strategic direction of the world energy transformation and power transformation, and an important strategic measure to deal with the global energy shortage and reduce environmental pollution [2]. The working principle of PEMFC is shown in fig 1.

* Corresponding author, e-mail: guancong2008@gmail.com

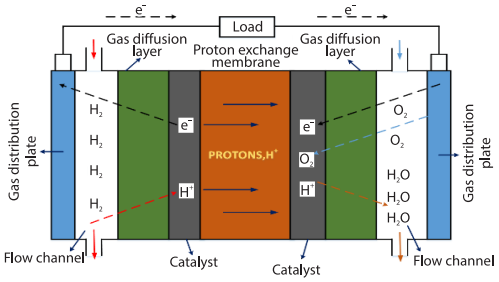

Figure 1. Fundamental diagram of PEMFC

Due to its characteristics of multi-variable, strong coupling and non-linear, traditional modelling methods are difficult to capture the PEMFC performance. In general, the complex systems are transformed into non-linear multidimensional functions, and then intelligent algorithms are used to solve the optimal value problems. The search ability and solving ability of the adopted optimization algorithm determine the accuracy of the model parameter identification. In recent years, with the development of artificial intelligence technology, various optimization algorithms emerge one after another, providing various effective methods and means for solving complex optimization problems, such as manta ray foraging optimization (MRFO) algorithm [3, 4], grey wolf Optimization algorithm [5], genetic algorithm [6], PSO algorithm [7, 8], whale optimization algorithm (WOA) [9], and differential evolution (DE) algorithm [10-12], *etc.* These methods and means can solve and optimize the complex models, but there are still problems in accuracy, speed and stability. Traditional methods such as DE algorithm and PSO are prone to premature phenomenon and fall into local optimum, so it is difficult to ensure the accuracy of the results. In order to solve the problem of premature convergence of the algorithm and improve the global search ability, various research work has been carried out. Zhong and Peng [13] proposed a dual-strategy improved DE algorithm to improve the global performance of DE algorithm. Tan *et al.* [14] introduced deep network to select mutation strategies by means of deep reinforcement learning. Zhao *et al.* [15] proposed a DE algorithm with neighboring mutation operator and opposition learning, which introduced new evaluation parameters and weight coefficients to replace large-scale global variation with higher search efficiency.

In order to solve the previous problems and make the model more accurate, this study proposed a hybrid PSO algorithm based on DE, which combines the strong global search ability of PSO algorithm with the characteristics of rapid convergence and high robustness of DE algorithm. Considering that different mutation strategies have impacts on the accuracy and convergence of the algorithm, this study selects the appropriate mutation strategy based on ranking. Meanwhile, with the purpose of further improve the searching ability and solving accuracy of hybrid DEPSO algorithm, a search strategy based on Levy flight is employed.

Mathematic model of PEMFC

The PEMFC generate liquid water when fully reactive, with a standard potential of 1.229 V. The actual output voltage is influenced by three main aspects: activation overvoltage, ohmic overvoltage and concentration overvoltage. Therefore, the output voltage of the PEMFC can be expressed as [5]:

$$V_{\text{cell}} = E_{\text{Nernst}} - V_{\text{act}} - V_{\text{ohmic}} - V_{\text{con}} \tag{1}$$

If n single cells are connected in series, the voltage of stack is:

$$V_{\text{stack}} = nV_{\text{cell}} \tag{2}$$

According to the equilibrium equation of hydrogen-oxygen reaction, the Nernst equation, which calculates the thermodynamic potential, can be given [6]:

$$E_{\text{Nernst}} = 1.229 - 0.85 \cdot 10^{-3}(T - 298.15) + 4.3085 \cdot 10^{-5} T \left[\ln(P_{\text{H}_2}) + \frac{1}{2\ln(P_{\text{O}_2})} \right] \tag{3}$$

where constant 1.229 is the standard potential, V, at 25 °C, P_{H_2} and P_{O_2} are the effective partial pressures of H_2 and O_2 of PEMFC, respectively.

If the reactants are air and hydrogen, the partial pressure P_{O_2} can be obtained from eq. (4). If the reactants are oxygen and hydrogen, P_{O_2} is obtained using eq. (5) [6-9]:

$$P_{O_2} = P_c - RH_c \cdot P_{H_2O} - \left(\frac{0.79}{0.21}\right) P_{O_2} \exp\left[0.291\left(\frac{i}{A}\right) T^{-0.832}\right] \tag{4}$$

$$P_{O_2} = RH_c \cdot P_{H_2O}^{sat} \left[\left(\exp\left(\frac{4.192\frac{i_{cell}}{A}}{T^{1.334}}\right)\frac{RH_a \cdot P_{H_2O}^{sat}}{P_c}\right)^{-1} - 1\right] \tag{5}$$

where RH_a and RH_c are the relative humidity of anode and cathode vapors, respectively, P_a and P_c – the input pressure of anode and cathode, A – the active area of the PEMFC, and $P_{H_2O}^{sat}$ – the saturation pressure of water vapor, which is a function of the operating temperature, T, and can be expressed:

$$\log(P_{H_2O}^{sat}) = 2.95 \cdot 10^{-2}(T - 273.15) - 9.18 \cdot 10^{-5} \cdot (T - 273.15)^2 + 1.44 \cdot 10^{-7}(T - 273.15)^3 - 2.18 \tag{6}$$

The activation loss is caused by the activation polarization of the cell, and this part of the voltage loss is used to activate the electrochemical reaction. This loss is calculated:

$$V_{act} = \xi_1 + \xi_2 T + \xi_3 T \ln(C_{O_2}) + \xi_4 T \ln(i_{cell}) \tag{7}$$

where ξ_i (i =1...4) is the semi-empirical coefficients and C_{O_2} – the concentration of dissolved oxygen at the cathode can be calculated by the formula:

$$C_{O_2} = \frac{P_{O_2}}{[5.08 \cdot 10^6 \exp(-498/T)]} \tag{8}$$

The ohmic overvoltage loss is mainly caused by the electric potential generated by the impedance of protons passing through the proton exchange membrane and the equivalent membrane impedance to proton transfer.

The voltage drop caused by ohmic loss is proportional to the current density, which can be obtained from the equation:

$$V_{ohmic} = i(R_M + R_C) \tag{9}$$

where R_C is the equivalent resistance of electron transfer, usually considered as constant and R_M – the equivalent resistance of membrane to proton movement, and the calculation formula:

$$R_M = \frac{\rho_M L}{A} \tag{10}$$

where L is the exchange membrane thickness and ρ_M – the resistivity of electron flow, which can be calculated by the method mentioned in [5]:

$$\rho_M = \frac{181.6\left[1 + 0.03\left(\frac{i}{A}\right) + 0.062\left(\frac{T}{303}\right)^2\left(\frac{i}{A}\right)^{2.5}\right]}{\left[\lambda - 0.634 - 3\left(\frac{i}{A}\right)\right]\exp\left[4.18\frac{T-303}{T}\right]} \tag{11}$$

where λ is a parameter related to gas humidity of the membrane.

Concentration differential pressure drop V_{con} is generated due to the change of reactant concentration and is calculated:

$$V_{con} = -B\ln\left(1-\frac{J}{J_{max}}\right) \tag{12}$$

where B is a coefficient parameter that depends on operation state, J – the current density, and J_{max} – the maximum current density.

Optimization method

Fitness function definition

There are some unknown parameters in the mathematical functions of the PEMFC model, which will affect the accuracy of fuel cell model prediction, thus it is necessary to identify the parameters properly. For determining the optimal value of parameters and make the model more accurate, the minimization of the sum of squares error between the measured voltage and the estimated output voltage is used as the optimization objective function. From the aforementioned description, the following formulae can be obtained:

$$s.t\begin{cases}\min f(x) = \min\left\{\sum_{k=1}^{k}\left(V_m - V_e\right)^2\right\}\\ \xi \le \xi_1 \le \xi_{i,\max}, \forall i = 1,2,3,4\\ \lambda_{\min} \le \lambda \le \lambda_{\max}\\ R_{C,\min} \le R_C \le R_{C,\max}\\ B_{\min} \le B \le B_{\max}\end{cases} \tag{13}$$

where k is the number of samples, V_m – the actual measured voltage of the PEMFC, and V_e – the output value. The objective function of optimization is the function of the unknown parameters ξ_1, ξ_2, ξ_3, ξ_4, λ, R_C, and B.

According to the description of the [16-18], the limits of parameters range are shown in tab. 1.

Table 1. Ranges of parameters

Parameters	ξ_1	ξ_2	ξ_3	ξ_4	λ	R_C	B
Lower limit	–1.1996	0.001	$3.6 \cdot 10^{-5}$	$-2.60 \cdot 10^{-4}$	10	0.0001	0.0136
Upper limit	–0.8532	0.005	$9.8 \cdot 10^{-5}$	$-9.54 \cdot 10^{-5}$	24	0.0008	0.5000

Improved algorithm

Kennedy and Eberhard [19] first proposed PSO in IEEE international conference on neural networks. The PSO algorithm has good performance in solving optimization problems, but it also has some shortcomings, such as slow convergence speed, low accuracy, easy to fall into local optimal. The DE algorithm has good convergence, but its accuracy is still deficient. In DE algorithm, different mutation strategies of parent vector will generate different mutation vectors, and a single invariant mutation strategy will generate different mutation vectors for different parent vectors. Based on the aforementioned points, this paper proposed hybrid DEPSO with the following specific strategies:

– Particle swarm search strategy based on Levy flight.

– Mutation strategy based on rank selection model.
– Hybrid PSO algorithm with DE.

Particle swarm search strategy based on Levy flight

In PSO, the position of the $i + 1$ particle is determined by the velocity and position of i^{th} particle. These particles are initially randomly and uniformly distributed throughout the search space. Then, they share their position continuously, and finally get the optimal solution. The diversity of population determines the global search capability of the algorithm, and PSO is prone to local convergence and premature phenomenon. Therefore, inspired by Levy flight trajectory [20, 21], a particle swarm search strategy is proposed in this paper:

$$x_i^{t+1} = x_i^t - \oplus \text{Levy}(\delta) \tag{14}$$

where x_i^{t+1} is the position of i^{th} particle in the $t + 1$ iteration, $\oplus$ – thepoint-to-point multiplication, and Levy(δ) – the random search path, which is obtained.

$$Levy(\delta) \sim 0.01 \frac{u}{|v|^{1/\delta}} (x_i - x_{i\text{best}}) \tag{15}$$

where the range of δ is (1, 3), $X_{i\text{best}}$ – the optimal position of the particle, and U and V – the conform to the normal distribution as shown:

$$u \sim N(0, \delta_u^2),\ v \sim (0, \delta_v^2) \tag{16}$$

The values of δ_u^2 and δ_v^2 are:

$$\delta_u = \left\{ \frac{\Gamma(1+\beta)\sin(pi\beta)}{\Gamma\left(\frac{1+\beta}{2}\right)\beta 2^{(\beta-1)/2}} \right\} 1/\beta, \delta_v = 1 \tag{17}$$

where β is a control parameter that follows normal distribution. At this moment, the particle swarm will record the optimal position found, update the current position, and repeat the previous behavior until a particle in the swarm reaches the set precision or the maximum number of iterations T.

Mutation strategy based on rank selection model

During the mutation operation of DE algorithm, many different mutation strategies have been proposed [16-18]:

– The DE/rand/1

$$v_{i,j}^t = x_{r1,j}^t + F\left(x_{r2,j}^t - x_{r3,j}^t\right) \tag{18}$$

– The DE/best/1

$$v_{i,j}^t = F_{\text{best}} + F(x_{r1,j}^t - x_{r2,j}^t) \tag{19}$$

– The DE/rand-to-best/1

$$v_{i,j}^t = x_{r1,j}^t + F\left(F_{\text{best}} - x_{r2,j}^t\right) \tag{20}$$

– The DE/best/2

$$v_{i,j}^t = F_{\text{best}} + F\left(x_{r1,j}^t - x_{r2,j}^t\right) + F\left(x_{r3,j}^t - x_{r4,j}^t\right) \tag{21}$$

– The DE/rand/2

$$v_{i,j}^{t} = x_{r1,j}^{t} + F\left(x_{r2,j}^{t} - x_{r3,j}^{t}\right) + F\left(x_{r4,j}^{t} - x_{r5,j}^{t}\right) \tag{22}$$

In general, the five random numbers r_1, r_2, r_3,r_4 , and r_5 in eks. (18)-(22) are randomly selected from the parent vector, which leads to the possibility that excellent individuals may not be all selected. Therefore, excellent individuals have more opportunities to participate in crossover and selection operations through sorting and selection:

– Ranking strategy

The fitness values of each individual in the population from best to worst are ranked, as shown:

$$R_i = NP - i, \ \ i = 1, 2, ...NP \tag{23}$$

where R_i is the ranking value of the ith individual and NP – the size of the population.

– Selection strategy

$$P_i = \frac{R_i}{NP}, \ \ i = 1, 2, ...NP \tag{24}$$

where P_i is the probability of the i^{th} individual being selected in the population, and the higher ranking of the order means the higher probability to be selected.

Improved algorithm steps

The hybrid DEPSO combines the advantages of DE algorithm and PSO in fast convergence, and introduces Levy flight strategy to expand the global search capability and effectively avoid falling into premature convergence. The mutation strategy based on rank selection model is employed to make more excellent individuals selected. The steps are as follows, as shown in fig. 2:

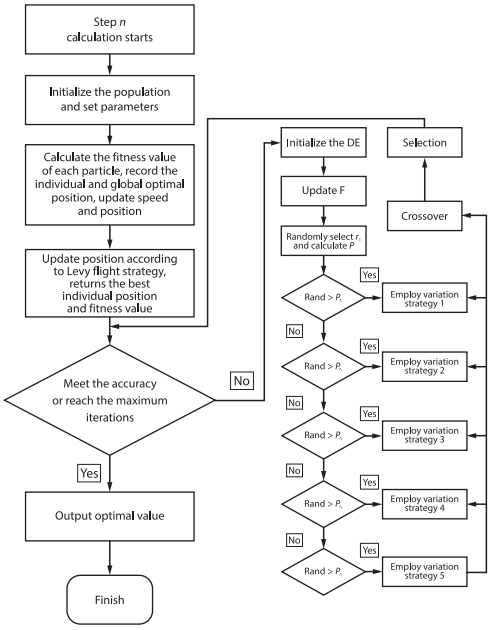

Figure 2. Flowchart of the hybrid DEPSO

– set the population size, dimension, iteration times, values of parameters *CR, NP,* C_1, C_2, initial position and speed of initialization population,
– calculate the fitness of each particle, record the individual optimal position and the global optimal position of the population, and update the individual velocity and position according to levy flight strategy by using eqs. (20)-(23),
– compare the optimal location of the individual with the optimal location of the population, update the optimal location of the population, returning the location and fitness value of the best individual, and
– judge whether the preset accuracy is reached, if so, output the result, otherwise, run the differential evolution algorithm to select and cross-operate the mutation strategy until the accuracy requirement is met or the maximum number of iterations is reached.

Algorithm testing and analysis

Six benchmark functions including Ackley, Griewank, Rastrigin, Rosenbrock, Schwefel, and Sphere are used in this study to verify the effectiveness and superiority of the algorithm. In order to increase the reliability of the algorithm, DE, PSO, MRFO, WOA, and hybrid DEPSO proposed in this paper are used to test these functions. The population size, maximum number of iterations, and dimension are the same in all algorithms, where in specific the population size $NP = 50$, the maximum iteration $T = 1000$, and the dimension $D = 30$.

Under the condition that the initial population size remains unchanged, the five algorithms are independently run for 20 times, and the test results are shown in tab. 2. The convergence curves of the six test functions are given in figs. 3-8. From figs. 3, 7, and 8, it can be clearly seen that hybrid DEPSO algorithm has fast convergence speed on Ackley, Schwefel, and Sphere functions, that is, the convergence can be completed within 300 generations, and it has a good convergence accuracy in the later stage. Figure 4 shows that there is little difference between hybrid DEPSO algorithm and WOA algorithm in solving accuracy, but hybrid DEPSO algorithm has faster convergence speed than WOA in the early stage. As indicated in fig. 5, the convergence speed of MRFO algorithm is better than that of hybrid DEPSO algorithm, but the solving accuracy becomes worse in the later stage. At this time, DE algorithm completes convergence around 300 generations, but the accuracy is not high, which may be due to falling into the local optimal value. As can be seen from fig. 6, except WOA algorithm, the other four algorithms have little difference in convergence speed, which are MRFO, PSO, DE, and hybrid DEPSO in sequence. From the point of view of solving accuracy, the order is MRFO, hybrid DEPSO, DE, and PSO. To sum up, the improved algorithm proposed in this study greatly improves the global search ability and optimization ability of the original algorithm.

Table 2. Mean and STD on six functions

Function		MRFO	WOA	DE	PSO	Hybrid DEPSO
Ackley	Mean	$5.6351 \cdot 10^{-15}$	$7.9936 \cdot 10^{-15}$	$3.2863 \cdot 10^{-14}$	$1.8652 \cdot 10^{-14}$	$8.8818 \cdot 10^{-16}$
	STD	$2.7486 \cdot 10^{-15}$	$3.6142 \cdot 10^{-15}$	$4.3521 \cdot 10^{-14}$	$1.8208 \cdot 10^{-13}$	$5.6351 \cdot 10^{-15}$
Griewank	Mean	$1.0311 \cdot 10^{+00}$	$1.8371 \cdot 10^{-02}$	$9.8647 \cdot 10^{-03}$	$9.8573 \cdot 10^{-03}$	$6.0348 \cdot 10^{-03}$
	STD	$1.0599 \cdot 10^{+00}$	$1.8914 \cdot 10^{-02}$	$5.6211 \cdot 10^{-02}$	$1.2625 \cdot 10^{-03}$	$7.5231 \cdot 10^{-03}$
Rastrigin	Mean	$5.1159 \cdot 10^{-13}$	$5.4557 \cdot 10^{-09}$	$2.4874 \cdot 10^{+01}$	$6.6501 \cdot 10^{-12}$	$5.6843 \cdot 10^{-14}$
	STD	$9.0381 \cdot 10^{-12}$	$1.1499 \cdot 10^{-09}$	$2.4876 \cdot 10^{+01}$	$1.4268 \cdot 10^{-11}$	$2.2737 \cdot 10^{-13}$
Rosenbrock	Mean	$1.9034 \cdot 10^{+01}$	$2.4918 \cdot 10^{+01}$	$2.7228 \cdot 10^{+01}$	$2.7150 \cdot 10^{+01}$	$2.3216 \cdot 10^{+01}$
	STD	$2.3412 \cdot 10^{+01}$	$1.4367 \cdot 10^{+02}$	$2.7759 \cdot 10^{+01}$	$2.7586 \cdot 10^{+01}$	$2.1363 \cdot 10^{+01}$
Schwefel	Mean	$-6.8430 \cdot 10^{+03}$	$-6.2410 \cdot 10^{+03}$	$-5.600 \cdot 10^{+03}$	$-6.627 \cdot 10^{+03}$	$-8.1270 \cdot 10^{+03}$
	STD	$-5.9575 \cdot 10^{+03}$	$-3.6988 \cdot 10^{+03}$	$-6.6365 \cdot 10^{+03}$	$-5.5868 \cdot 10^{+03}$	$-8.0641 \cdot 10^{+03}$
Sphere	Mean	$1.9093 \cdot 10^{-180}$	$5.4359 \cdot 10^{-60}$	$3.4251 \cdot 10^{-12}$	$4.2184 \cdot 10^{-190}$	$3.2395 \cdot 10^{-263}$
	STD	$2.8501 \cdot 10^{-85}$	$7.1039 \cdot 10^{-45}$	$1.9100 \cdot 10^{-08}$	$6.2980 \cdot 10^{-89}$	$2.5145 \cdot 10^{-83}$

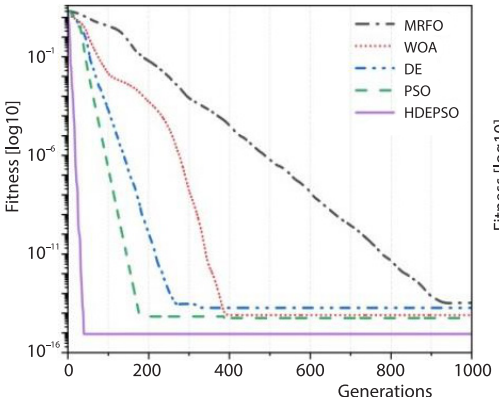

Figure 3. The convergence curve of Ackley

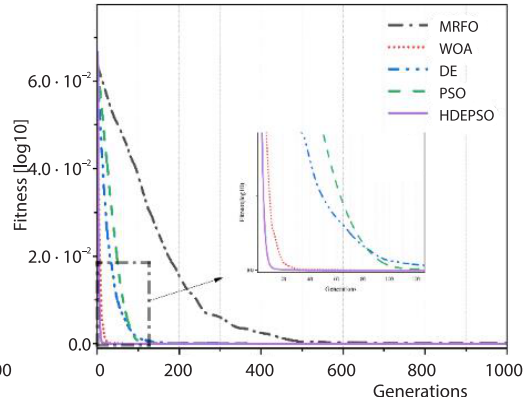

Figure 4. The convergence curve of Griewank

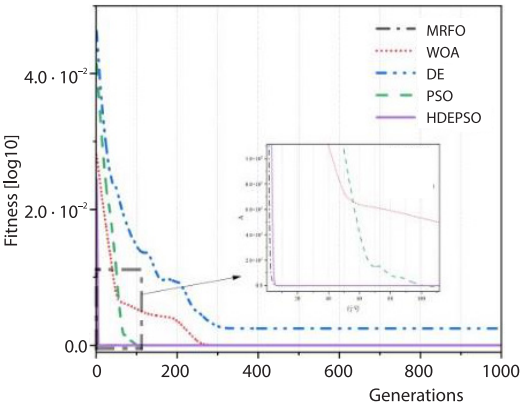

Figure 5. The convergence curve of Rastrigin

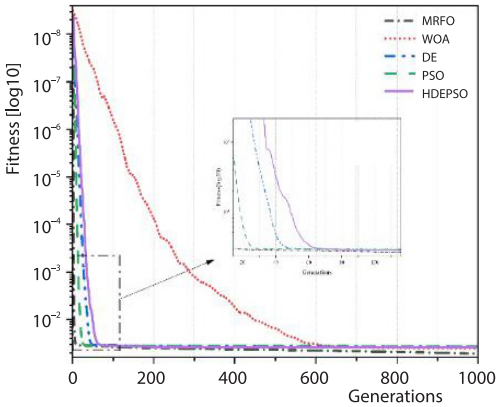

Figure 6. The convergence curve of Rosenbrock

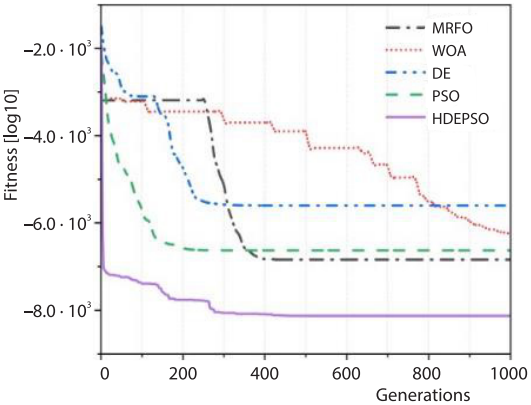

Figure 7. The convergence curve of Schwefel

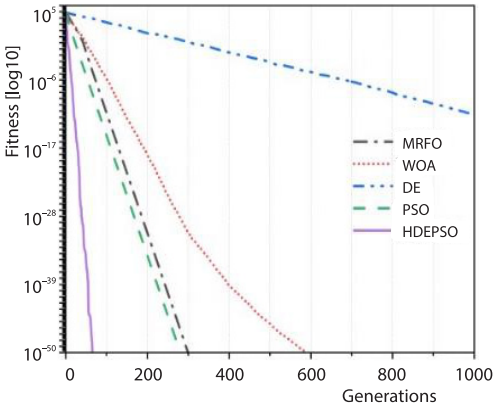

Figure 8. The convergence curve of Sphere

Simulation and verification

Some parameters in the PEMFC model cannot directly solve the gradient and other related information. In the previous section, this study adopts the hybrid differential PSO algorithm for parameter identification and verifies the effectiveness of the algorithm. For eqs. (1)-(13) of the PEMFC mathematical model, this study conducted simulation verification under the environment of Intel(R) Core (TM) I7-8550U CPU 1.80 GHz and software MATLAB2018b.

In this section, in order to test the effect of the algorithm in practice, two stacks are used to verify the simulation results of the algorithm. The stacks are 3 kW, 80 kW, respectively.

Case study 1 (3 kW PEMFC)

Table 3 shows some parameters and operating environment of PEMFC rated at 3 kW. In order to compare the performance of hybrid DEPSO algorithm and other conventional algorithms, the values of unknown parameters obtained by the five algorithms are shown in tab. 4. At the same time, the optimal fitness value of each algorithm SSE is also given in the table. From tab. 4, the SSE value of hybrid DEPSO algorithm proposed in this study is smaller and has higher accuracy. The simulation model verifies that when the hybrid DEPSO algorithm achieves the optimal fitness, it is exactly the minimum SSE value between the measured voltage and the predicted voltage. The trend of convergence is shown in fig. 9(a), and polarization curves of DE, PSO, and hybrid DEPSO algorithms are shown in fig. 9(b). As can be seen from the aforementioned two figures, each algorithm is able to converge within 100 generations. The hybrid DEPSO algorithm has the highest convergence precision, while the WOA algorithm is the lowest. Secondly, hybrid DEPSO algorithm has the highest fitting accuracy, followed by DE, and MRFO is the worst. In the actual operation process, the weight of active polarization voltage drop is not as large as that in the model, thus each algorithm will have some deviation, which may be caused by the error of PEMFC model. Figure 9(c) is the error box plot of the algorithm, in which the median error line and mean value of MRFO and hybrid DEPSO algorithms are consistent. It can be seen from the figure that the mean error of hybrid DEPSO is around 0.01, and the accuracy is 0.19-1.86% higher than that of others (calculated in tab. 5).

Table 3. The characteristics of the PEMFC (3 kW)

Technical specification	
Type of fuel cell	PEM
Rated power	3 kW
Ambient temperature	25 °C
Coolant	Air
Reactants	Hydrogen and air
T_{stack}	353 K
J_{max}	1 A/cm^2
R_{H_2}	60%
R_{O_2}	40%
n	5
A	100 cm^2
P_a	1.5 bar
P_c	0.21 bar

Table 4. Comparison of optimal results of three algorithms

Parameters	MRFO	WOA	DE	PSO	Hybrid DEPSO
ξ_1	–0.9440	–0.9490	–0.9543	–0.9482	–0.9494
ξ_2	0.0034	0.0031	0.0031	0.0032	0.0030
ξ_3	$7.40 \cdot 10^{-05}$	$7.44 \cdot 10^{+02}$	$7.40 \cdot 10^{-05}$	$7.44 \cdot 10^{-05}$	$7.45 \cdot 10^{-05}$
ξ_4	–1.98E-04	$-1.92 \cdot 10^{-04}$	$-1.95 \cdot 10^{-04}$	$-1.88 \cdot 10^{-04}$	$-1.89 \cdot 10^{-04}$
R_c	$1.32 \cdot 10^{-04}$	$1.32 \cdot 10^{-04}$	$1.33 \cdot 10^{-04}$	$1.33 \cdot 10^{-04}$	$1.33 \cdot 10^{-04}$
λ	23.14	19.99	20.33	21.43	20.22
B	0.0362	0.0327	0.0319	0.0338	0.0325
SSE	$4.44 \cdot 10^{-02}$	$4.99 \cdot 10^{+00}$	$4.43 \cdot 10^{-02}$	$4.45 \cdot 10^{-02}$	$4.28 \cdot 10^{-02}$

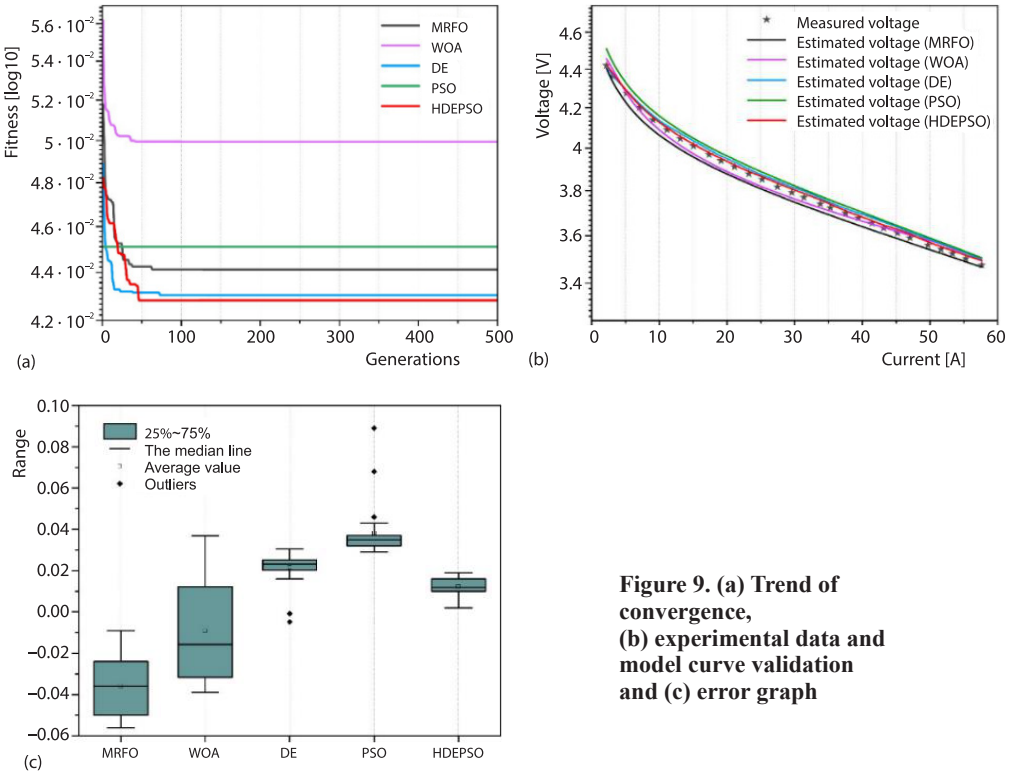

Figure 9. (a) Trend of convergence, (b) experimental data and model curve validation and (c) error graph

According to the comparison between the measured data and the simulation data obtained by the five algorithms in tab. 5, it can be seen that among the five algorithms, the hybrid DEPSO algorithm proposed in this study is higher in accuracy than the other algorithms. Secondly, it can be seen from fig. 9(a) that the hybrid DEPSO algorithm has reached the optimal fitness value before the 20th generation. To sum up, hybrid DEPSO algorithm combines the advantages of DE and PSO optimization algorithms, and can avoid local optimal while completing fast optimization.

Case study 2 (80 kW PEMFC)

The measured data of this case comes from a company in Wuhan. See tab. 6 for specific parameters. Four test cases of 3 bar/353 K, 1.5 bar/353 K, 3 bar/335 K, and 1.5 bar/335 K

Table 5. Estimated data and measured voltage data

Measured data		MRFO	WOA	DE	PSO	Hybrid DEPSO
$I_{mea}(A)$	$V_{mea}(V)$					
57.656	3.475	3.466	3.473	3.495	3.505	3.493
55.311	3.502	3.488	3.506	3.526	3.531	3.516
53.333	3.523	3.507	3.535	3.547	3.553	3.535
51.648	3.541	3.524	3.562	3.566	3.571	3.552
49.705	3.559	3.542	3.582	3.586	3.593	3.572
47.043	3.590	3.568	3.608	3.613	3.622	3.608
45.207	3.611	3.587	3.627	3.637	3.643	3.627
43.141	3.633	3.607	3.648	3.658	3.666	3.644
41.436	3.654	3.624	3.666	3.679	3.686	3.666
39.434	3.677	3.645	3.687	3.698	3.709	3.687
37.539	3.698	3.665	3.708	3.719	3.731	3.708
35.287	3.723	3.689	3.722	3.746	3.757	3.739
33.802	3.740	3.705	3.749	3.767	3.775	3.759
31.375	3.769	3.732	3.787	3.799	3.805	3.787
29.588	3.792	3.752	3.808	3.816	3.828	3.808
27.463	3.818	3.778	3.835	3.845	3.855	3.835
25.197	3.852	3.806	3.864	3.871	3.886	3.864
23.238	3.878	3.832	3.889	3.899	3.913	3.889
21.124	3.911	3.861	3.919	3.933	3.945	3.919
19.126	3.939	3.890	3.950	3.961	3.976	3.950
17.368	3.969	3.917	3.978	3.992	4.005	3.978
15.068	4.010	3.956	4.018	4.034	4.047	4.018
13.114	4.046	3.993	4.056	4.073	4.085	4.056
11.146	4.089	4.035	4.098	4.107	4.129	4.098
9.085	4.138	4.085	4.150	4.158	4.181	4.149
7.058	4.201	4.145	4.211	4.218	4.244	4.210
5.124	4.273	4.218	4.284	4.289	4.319	4.285
3.146	4.361	4.325	4.393	4.360	4.429	4.377
2.184	4.419	4.403	4.441	4.414	4.508	4.421

were adopted. The algorithm was independently run for 30 times to verify the performance curve of PEMFC. Figure 10(a) compares the simulation results with the experimental data by changing the working temperature under the condition that the partial pressures of hydrogen and oxygen remain unchanged. Figure10(b) shows the volt-ampere curves of PEMFC obtained by changing the partial pressures of oxygen and hydrogen at the same operating temperature. It can be seen that the output voltage and current characteristics of the PEMFC model are basically consistent with the experimental data.

Table 6. The characteristics of the PEMFC(80 kW)

Technical specification	
Type of fuel cell	PEM
Rated power	80 kW
Ambient temperature	25 °C
Coolant	Water
Reactants	Hydrogen and air
T_{stack}	353 K
J_{max}	1.40 A/cm^2
R_{H_2}	80%
R_{O_2}	60%
n	300
A	350 cm^2
P_a	1.50 bar
P_c	1.50 bar

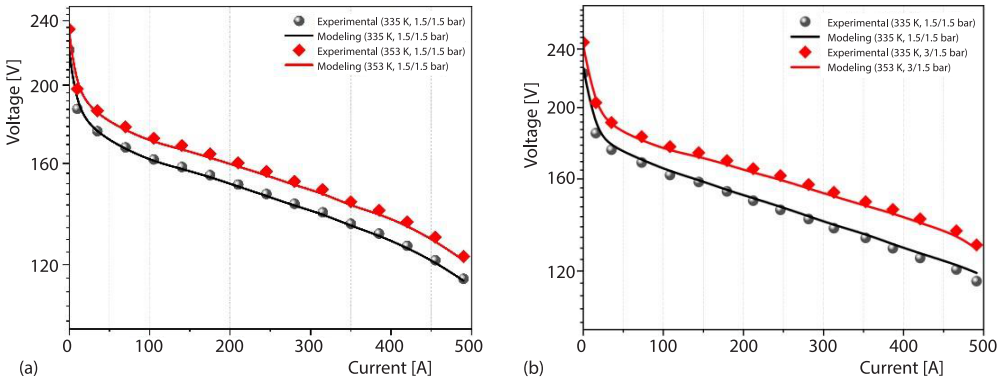

Figure 10. Case study 2: The comparative curve of experimental and modelling data for different temperature and pressures; (a) different temperature and (b)different pressures

The error of voltage value obtained by proposed algorithm may be caused by a small amount of hydrogen at the anode infiltrating from the proton exchange membrane to the cathode, a small amount of electrons flowing through the proton exchange membrane to the outside, poor insulation and other factors. Therefore, a part of the current of PEMFC is not calculated in the mathematical model, resulting in the errors. Secondly, the PEMFC used in this experimental case uses water as coolant, and the temperature difference between the inlet and outlet of cooling water is between 0.3-3 °C, and the internal temperature is not easy to measure. However, the proposed algorithm adopts a mathematical model under ideal conditions, which may lead to errors between measured data and simulation data. But in general, the hybrid DEPSO algorithm proposed in this study is effective for parameter identification of PEMFC model.

Conclusions

In order to identify uncertain parameters of PEMFC model in the non-linear steady-state system, this paper proposes a novel hybrid DEPSO algorithm, which has the following three major contributions.

- The hybrid DEPSO algorithm combines the advantages of many strategies to realize effective and reliable parameter identification of PEMFC.
- The effectiveness and feasibility of hybrid DEPSO algorithm in PEMFC parameter identification are evaluated, and compared with that of other four typical algorithms.
- Three case studies of 3 kW, 80 kW stacks were carried out to verify that hybrid DEPSO can significantly improve the accuracy, convergence speed and stability of PEMFC parameter identification under different operating conditions. In specific, the accuracy of parameter identification of hybrid DEPSO can be improved by 51.49%, 86.42%, 59.12%, and 43.47% in comparison with that of MRFO, WOA, DE, and PSO, respectively.

Nevertheless, in the process of research, we found that the proposed method still exists some limitations, for instance the hybrid DEPSO adopts mathematical model of PEMFC under ideal conditions, and better results may be obtained by incorporating the influence of leakage current into the model. In conclusion, the hybrid DEPSO algorithm has superiority for solving multi-objective optimization problems, which will be applied for solving other similar collaborative optimization problems of engineering models.

Acknowledgment

The project is supported by the National Natural Science Foundation of China (51909200), the International S&T Cooperation Program of China (2019YFE0104600), and the National Key Research and Development Program of China (2019YFB1504703)

Nomenclature

A – active area of the PEMFC
B – coefficient parameter
C_{O_2} – concentration of dissolved oxygen
i – current
J – current density
J_{max} – maximum current density
L – thickness of exchange membrane
NP – size of the population
P_a, P_c – input pressure of anode and cathode
P_{H_2} – effective partial pressures of H_2
P_{O_2} – effective partial pressures of O_2
$P_{H_2O}^{sat}$ – saturation pressure of water vapor
R_C – equivalent resistance of electron transfer
RH_a, RH_c – relative humidity of anode and cathode vapors
R_i – ranking value of the ith individual
R_M – equivalent resistance of membrane to proton movement
r_1, r_2, r_3, r_4, r_5 – Random numbers
T – temperature
V_{act} – activation overvoltage
V_{cell} – output voltage
V_{con} – concentration overvoltage
V_{ohmic} – ohmic overvoltage
V_{stack} – voltage of stack

Greek symbols

λ – parameter related to gas humidity of the membrane
ξ_1, ξ_2, ξ_3, ξ_4, – semi-empirical coefficients
ρ_M – resistivity of electron flow

Subscripts

a – anode
act – activation
c – cathode
con – concentration
M – membrane
mea – measured
max – maximum
STD – standard

Superscript

sat – saturation

References

[1] Shaahid, S. M., *et al*., Techno-Economic Assessment of Establishment of Wind Farms in Different Provinces of Saudi Arabia to Mitigate Future Energy Challenges, *Thermal Science*, *23* (2019), 5B, pp. 2909-2918
[2] Riboldi, L., *et al*., The Impact of Process Heat on the Decarbonisation Potential of Offshore Installations by Hybrid Energy Systems, *Energies*, *14* (2021), 23, 8123
[3] Zhao, W., *et al*., Manta Ray Foraging Optimization: An Effective Bioinspired Optimizer for Engineering Applications, *Engineering Applications of Artificial Intelligence*, *87* (2020), 1, 103300
[4] Hemeida, M. G., Distributed Generators Optimization Based on Multi-Objective Functions Using Manta Rays Foraging Optimization Algorithm (MRFO), *Energies*, *13* (2020), 7, pp. 564-572
[5] Miao, D., *et al*., Parameter Estimation of PEM Fuel Cells Employing the Hybrid Grey Wolf Optimization Method, *Energy*, *193* (2020), 11, pp. 116616
[6] Čongradac, V. D., *et al*., Control of the Lighting System Using a Genetic Algorithm, *Thermal Science*, *16* (2012), 1, pp. 237-250
[7] Li, Q., *et al*., Adoption of Computer Particle Swarm Optimization Algorithm under Thermodynamic Motion Mechanism, *Thermal Science*, *24* (2020), 5A, pp. 2707-2715
[8] Askarzadeh, A., Alireza, R., Optimization of PEMFC Model Parameters with a Modified Particle Swarm Optimization, *International Journal of Energy Research*, *35* (2011), 11, pp. 1258-1265
[9] El-Fergany, A. A, *et al*., Semi-Empirical PEM Fuel Cells Model Using Whale Optimization Algorithm, *Energy Conversion and Management*, *201* (2019), 12, pp. 1-11
[10] Sun, W., Yi, L., Research of Least Squares Support Vector Regression Based on Differential Evolution Algorithm in Short-Term Load Forecasting Model, *Journal of Renewable and Sustainable Energy*, *6* (2014), 5, 053137
[11] Qin, A. K., *et al*., Differential Evolution Algorithm with Strategy Adaptation for Global Numerical Optimization, *IEEE Transactions on Evolutionary Computation*, *13* (2009), 5, pp. 398-417
[12] Sarajlić, M., *et al*., Identification of the Heat Equation Parameters for Estimation of a Bare Overhead Conductor's Temperature by the Differential Evolution Algorithm, *Energies, 11* (2018), 8, 2061
[13] Zhong, X., Peng, C., An Improved Differential Evolution Algorithm Based on Dual-Strategy, *Mathematical Problems in Engineering*, *2020* (2020), 11, pp. 1-14
[14] Tan, Z., Li, K., Differential Evolution with Mixed Mutation Strategy Based on Deep Reinforcement Learning, *Applied Soft Computing*, *111* (2021), 7, 107678
[15] Zhao, W., *et al*., Manta Ray Foraging Optimization: An Effective Bioinspired Optimizer for Engineering Applications, *Engineering Applications of Artificial Intelligence*, *87* (2020), 1, 103300
[16] Yang, B., *et al*., Parameter Identification of Proton Exchange Membrane Fuel Cell Via Levenberg-Marquardt Backpropagation Algorithm, *International Journal of Hydrogen Energy*, *46* (2021), 5
[17] Gong, W., Cai, Z., Accelerating Parameter Identification of Proton Exchange Membrane Fuel Cell Model with Ranking-Based Differential Evolution, *Energy, 59* (2013), 9, pp. 356-364
[18] Sun, Z., *et al.* Parameter Identification of PEMFC Model Based on Hybrid Adaptive Differential Evolution Algorithm, *Energy, 90* (2015),7, pp. 1334-1341
[19] Kennedy, J., Eberhart, R., Particle Swarm Optimization, *Proceedings,* IEEE International Conference On Neural Networks, Perth, Australia, Vol. 4, 1995, pp. 1942-1948
[20] Chechkin, A. V., *et al.,* Introduction the Theory of Levy Flights, in: *Anomalous Transport: Foundations* (ed. Klages *et al.*), Wiley-VCH, Weinheim, Germany, 2008, 129-162
[21] Ling, Y., *et al*., Levy Flight Trajectory-Based Whale Optimization Algorithm for Global Optimization, *IEEE Access, 5* (2017), 4, pp. 6168-6186
[22] Li, C., B., *et al*., Ecological Performance of an Irreversible Proton Exchange Membrane Fuel Cell, *Science of Advanced Materials*, *8* (2020), 12, pp.

Paper submitted: September 12, 2022
Paper revised: February 9, 2023
Paper accepted: February 15, 2023